**A point-by-point response to reviewers**

Dear Editor,

We are very pleased to submit a revised manuscript entitled with “The density of ambient black carbon retrieved by a new method: implications to CCN prediction” for possible publication in journal of ACP.

I'd like to thank you for your efforts and time on handling the paper. I also would like to thank the reviewers for their valuable comments and suggestions, all of which have been considered carefully during the revision (a point-by-point response to reviewers as follows). We believe all the comments from the reviewers have been addressed, and the paper have been greatly improved after the revision.

Yours sincerely,

Fang Zhang

On behalf of all authors

**A point-by-point response to reviewer**

**Reviewer #1**

The manuscript presents a method for retrieving BC density and implications for CCN prediction. Since the BC density is difficult to measure, it is worth trying to develop new methods for retrieving accurate BC density from available measured data. It is quite interesting. However, more work needs to be done with the manuscript before it can be accepted.

It is not clear how the mixing state and the density of BC are retrieved based the description in the methodology section (2.2)?

- The definition of mixing state is especially not clear. What exactly the mixing state is referred to? Internal? External? Do the authors mean the mass size distributions for the internal and external BC?

Re: (1) To make it more clearly that how the mixing state and the density of BC are retrieved, we just have broken the section (2.2) to two parts section 2.2.1 and 2.2.2, to introduce the methods to retrieve the mixing state and density respectively (see the revised text).

And, regarding to the definition of BC mixing state, in this study, the BC mixing state refers to the heterogeneity of the BC aerosol population. Freshly emitted BC particles, are usually externally mixed in the atmosphere, however, they generally undergo aging processes by condensation, coagulation as well as oxidation (Ivleva et al., 2007; Peng et al., 2016) and gradually become internally mixed (coated) with other chemical components. Here, the number or mass concentration fraction of the internally mixed (coated) and externally mixed (uncoated) BC is respectively retrieved from the hygroscopic and hydrophobic mode of Gf-PDF measured by HTDMA system.

Some statements have been added in the revised text, see **Lines 60-69**, or as follows:

"… BC particles, with diesel vehicles, industrial and residential coal combustion as major sources, are ubiquitous in urban environments (Bond et al., 2013; Dameto et al., 2017; Li et al., 2017; Liu et al., 2019a). The mixing state of BC describes the distribution of the bare BC and coating masteries among the aerosol population. Typically, freshly generated BC exists in the form of chain aggregates and initially uncoated, which is known as externally mixed BC (Ex-BC). When the BC particles were emitted, they generally mix with other materials by condensation, coagulation, and other processes (Riemer et al., 2004; Zhang et al., 2008; Liu et al., 2013; Zhang et

al., 2020), forming the internally mixed BC (In-BC) particles consisting of BC core and other chemical components (Cheng et al., 2006; Zhang et al., 2016) …"

(2) In Section 2.2, the mass size distribution of externally mixed BC (Ex-BC) was fit using the log-normal distribution which was given in the references (Wu et al., 2017; Liu et al., 2019a; Zhao et al., 2022). Detailed description about the method to retrieve the mixing state of BC (the Ex-BC and In-BC) are given in **Lines 183-209,** or as follows:

"… By assuming that the particles are spherical (Rader and McMurry, 1986), the mass size distribution of Ex-BC ($M_{\text{Ex-BC}}$) was obtained as follows:

$$M_{\text{Ex-BC}}(\log Dp) = \frac{\pi}{6} {D_p}^3 \rho n_{\text{Ex-BC}}(\log Dp) \quad (5)$$

where $D_p$ is the mobility diameter, $\rho$ is the effective density of Ex-BC, and $n_{\text{Ex-BC}}$ (log $D_p$) is the function of the number size distribution of Ex-BC, respectively. By reviewing and summarizing the existing results about, we show that typical values of density for the freshly emitted or externally mixed BC observed in the winter of urban Beijing or North China Plain spans over 0.14-0.50 g cm$^{-3}$, with mean of ~0.40±0.10 g cm$^{-3}$ (Fig. S3), in the size range of 100 to 300 nm, where the mass concentration of externally mixed BC accounted for a large proportion in urban Beijing (Geller et al., 2006; Peng et al., 2016, 2017; Wu et al., 2019; Liu et al., 2020; Zhao et al., 2022). Therefore, an average $\rho_{\text{Ex-BC}}$ of 0.4 g cm$^{-3}$ was used for calculating the mass concentration of externally-mixed BC in our study. The uncertainty analysis exhibits that the variations of the $\rho_{\text{Ex-BC}}$ could lead to an average deviation of ±10 % in the calculating In-BC density (Fig. 2e) by increasing the $\rho_{\text{Ex-BC}}$ from 0.1 to 0.6 g cm$^{-3}$, showing a small impact on the retrieved result. Uncertainty analyses due to the variations of $\rho_{\text{Ex-BC}}$ were given in section 2.3.

The mass size distribution of Ex-BC was fit using the log-normal distribution as shown in Fig. S4 (Wu et al., 2017; Liu et al., 2019a; Zhao et al., 2022). Thus, the bulk mass concentration of Ex-BC can be calculated from the integration of the mass size distribution:

$$m_{\text{Ex-BC}} = \int_{D_{start}}^{D_{end}} M_{\text{Ex-BC}}(\log D_p)\ d\log(D_p) \quad (6)$$

$$m_{\text{In-BC}} = m_{\text{BC}} - m_{\text{Ex-BC}} \quad (7)$$

where $D_{\text{start}}$ and $D_{\text{end}}$ are the lower and upper size limit, $M_{\text{Ex-BC}}$ (log $D_p$) is the function of the Ex-BC mass size distribution. We then obtained the bulk mass concentration of internally mixed BC ($m_{\text{In-BC}}$) by subtracting $m_{\text{Ex-BC}}$ from the bulk BC mass

concentration measured by AE33 in equation 7 …"

- The density is calculated by equation 8, so in the calculations, there must be lots of assumptions for the relevant parameters. How each parameter in the equation is determined? Those need to be clearly described. It is obviously not well illustrated in the current version.

  Re: thanks a lot for the comments. In the revision, we just have clarified and added some illustrations for the relevant parameters in equation 8, and an uncertainty analysis of each assumed parameter has been done, see **Lines 210-347**, as follows (see Figs. R1 and R2):

  **"2.2.2 Retrieving the density of BC**

  For retrieval of the density of BC, the principal idea is to use the measured $\kappa_{gf}$ to calculate the density of BC based on the Zdanovskii–Stokes–Robinson (ZSR) mixing rule (Stokes and Robinson, 1966; Zdanovskii, 1948) with the chemical composition measured by AMS (Petters & Kreidenweis, 2007). In the retrieval, several aspects are concerned. First, since the ZSR rule is to assume the aerosol particles are internally mixed, the $\kappa_{gf}$ value of the more MH mode ($\kappa_{gf\text{-}MH}$) is thus applied for retrieving the density of internally mixed BC. Second, since the size distribution of BC number concentration is usually with peaks between 100 and 200 nm (Liu et al., 2019a; Yu et al., 2020; Zhao et al., 2022), the $\kappa_{gf\text{-}MH}$ value of particles in accumulation mode was averaged and applied for the retrieval. Previous studies showed an independence of $\kappa_{gf\text{-}MH}$ on particle size when the $D_p$ >100 nm during the campaign period (Fan et al., 2020). Therefore, the average of $\kappa_{gf\text{-}MH}$ in accumulation mode is reasonable for the determination of the In-BC density. In addition, because the inversion including measurements from HTDMA and HR-AMS, a total mass closure of the measured aerosol particles was conducted between the two techniques by comparing the mass concentration of $PM_1$ and the results are well consistent (Fig. S5). The density of internally mixed BC (In-BC), $\rho_{In\text{-}BC}$ is then derived from the following equations:

$$\kappa_{gf-MH} = \kappa_{chem} = \sum_i \varepsilon_i \kappa_i = \frac{v_{inorg}}{v_{total}} \kappa_{inorg} + \frac{v_{SOA}}{v_{total}} \kappa_{SOA} + \frac{v_{In-POA}}{v_{total}} \kappa_{POA} + \frac{v_{In-BC}}{v_{total}} \kappa_{BC} \quad (8)$$

  where $\kappa_{gf\text{-}MH}$ is the hygroscopic parameter of the more hygroscopic (MH) mode, $\kappa_{chem}$ is the hygroscopic parameter of aerosol particles in the mixed composition and can be calculated based on chemical volume fractions using a simple rule (Stokes and Robinson, 1966; Petters & Kreidenweis, 2007), $\kappa_i$ is the hygroscopic parameter of each

pure composition and $\varepsilon_i$ is the volume faction of the individual components in the internal-mixed particle. $v_{inorg}$, $v_{SOA}$ and $v_{In\text{-}POA}$ are the volume of the inorganic, SOA and internally mixed POA species, and can be calculated as follows: $v_{inorg} = \frac{m_{inorg}}{\rho_{inorg}}$, $v_{SOA} = \frac{m_{SOA}}{\rho_{SOA}}$, and $v_{In-POA} = \frac{m_{In-POA}}{\rho_{POA}}$. $v_{total}$ is the total volume of all the species and can be written as $v_{total} = \frac{m_{inorg}}{\rho_{inorg}} + \frac{m_{SOA}}{\rho_{SOA}} + \frac{m_{In-POA}}{\rho_{POA}} + \frac{m_{In-BC}}{\rho_{In-BC}}$. In equation (8), $\kappa_{BC}$ and $\kappa_{POA}$ are assumed to be 0. Then, the $\rho_{In\text{-}BC}$ can be calculated based on its mass concentration and volume as follows:

$$\rho_{In-BC} = \frac{m_{In-BC}}{\left(\frac{\frac{m_{inorg}}{\rho_{inorg}}\kappa_{inorg} + \frac{m_{SOA}}{\rho_{SOA}}\kappa_{SOA}}{\kappa_{gf-MH}} - \frac{m_{inorg}}{\rho_{inorg}} - \frac{m_{SOA}}{\rho_{SOA}} - \frac{m_{In-POA}}{\rho_{POA}}\right)} \quad (9)$$

where, $m_{In\text{-}BC}$ is the mass concentration of internally mixed BC, $m_{inorg}$ and $m_{SOA}$ are the mass concentrations of the inorganic species and SOA, which are measured by the AMS. $m_{In\text{-}POA}$ is the mass concentrations of internally mixed POA and can be calculated subtracting the mass fraction of NH-POA from the total mass concentrations of POA. $\rho_{inorg}$, $\rho_{SOA}$ and $\rho_{POA}$ are the density of the inorganic species, SOA and POA. Since the AMS measures the concentrations of the organic and inorganic ions, including $SO_4^{2-}$, $NO_3^-$, $NH_4^+$, $Cl^-$. Here inorganic species were derived by applying a simplified ion pairing scheme (Gysel et al., 2007) to convert mass concentrations of ions to the inorganic salts as follows:

$$n_{NH_4NO_3} = n_{NO_3^-}$$

$$n_{NH_4HSO_4} = \min(2n_{SO_4^{2-}} - n_{NH_4^+} + n_{NO_3^-}, n_{NH_4^+} - n_{NO_3^-})$$

$$n_{(NH_4)_2SO_4} = \max(n_{NH_4^+} - n_{NO_3^-} - n_{SO_4^{2-}}, 0)$$

$$n_{H_2SO_4} = \max(0, n_{SO_4^{2-}} - n_{NH_4^+} + n_{NO_3^-}) \quad (10)$$

where $n$ represents the number of moles, then the mass concentrations were obtained by the number of moles times the molar mass of each inorganic salts. Because the maximum value of the $n_{H_2SO_4}$ was zero in this campaign. Three inorganic salts including $NH_4HSO_4$, $(NH_4)_2SO_4$, and $NH_4NO_3$ were applied in our study. The densities for inorganic salts were taken from previous studies (Gysel et al., 2007; Wu et al., 2016). Here the densities for three inorganics are 1.78, 1.769 and 1.72 g $cm^{-3}$, respectively. By summarizing the previous studies (Gysel et al., 2007; Dinar et al., 2006), 1.4 g $cm^{-3}$ was

selected as the density of SOA ($\rho_{SOA}$). The density of POA ($\rho_{POA}$) is assumed to be 1.0 g $cm^{-3}$ for urban environments, which is similar to the lubricating oil (Wu et al., 2016). Considering the cooking organic aerosols represent a high contribution to POA in urban environments, a density of 0.85 g $cm^{-3}$ chosen as the mean density for the rapeseed oil and oleic acid (Reyes-Villegas et al., 2018) was also used to evaluated the result as shown in section 2.3. The values of $\kappa$ for inorganic components are 0.56 for $NH_4HSO_4$, 0.48 for $(NH_4)_2SO_4$ and 0.58 for $NH_4NO_3$, along with the best-fit values for the three inorganic salts (Petters & Kreidenweis, 2007 and Gunthe et al., 2009). The $\kappa_{SOA}$ is assumed to be 0.15 according to the field studies in urban areas (Chang et al., 2010; Kawana et al., 2016) …"

**"2.3 Uncertainties and limitations**

For the retrieval, the assumptions on the values of $\kappa_{SOA}$, $\rho_{POA}$, $\rho_{SOA}$ and $\rho_{Ex\text{-}BC}$ as well as the fraction of primary organic aerosols in non-hygroscopic or hygroscopic mode would add uncertainty in the inferred values of ambient internally mixed BC density. For example, the freshly emitted POA particles might consistently be coated with the secondary particles during the aging process, resulting in changes of the $NF_{NH\text{-}POA}$. However, a real-time variation of the $NF_{NH\text{-}POA}$ is not yet available due to the lack of such measurements data. Applying the rough fractions of hydrophobic POA only under three different atmospheric conditions could still cause uncertainties. Also, the densities of POA and SOA may differ due to their precursors, emission sources and the formation mechanisms in ambient atmosphere (Alfarra et al., 2006; Reyes-Villegas et al., 2018). And the density of Ex-BC is generally characterized by the morphology and size (Wu et al., 2019). In addition, the value of $\kappa_{SOA}$ spans largely due to the variability in the emissions of gas precursors and formation processes under different atmospheric conditions (Zhang et al., 2015; Liu et al., 2021b). Therefore, we examined the sensitivities of In-BC density to the variations of these factors, as exhibited in Fig. 1 and Fig.2.

The figures show that the In-BC density gradually decreases with the increment of the $NF_{NH\text{-}POA}$, implying the higher fraction of bare POA particles correspond to the early aging stage of aerosol particles. With increase of $\kappa_{SOA}$, the In-BC density is generally reduced, but with small fluctuations (Fig.1a, Fig. 2b). This suggests a complex impact of assumptions of $\kappa_{SOA}$ on the retrieved BC density. In addition, the In-BC density decreases very slightly as $\rho_{Ex\text{-}BC}$ increases (Fig. 2e), suggesting applying a larger $\rho_{Ex\text{-}BC}$ would derive smaller values for In-BC density. The In-BC density is insensitive to the

changes of the density of POA and SOA, showing an almost negligible effect on the retrieved results (Fig. 2c and d).

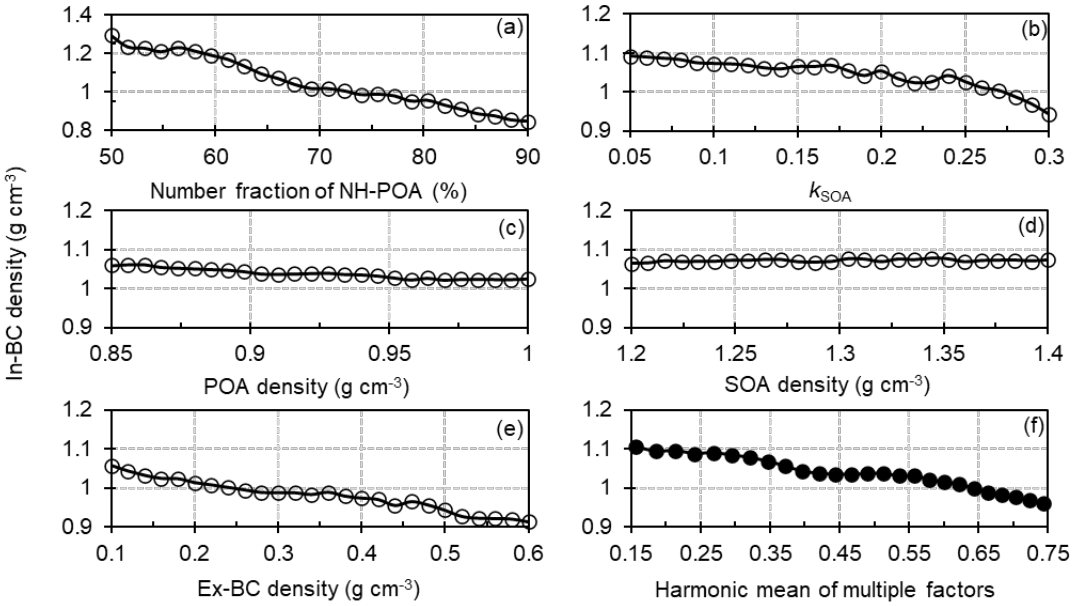


**Fig. R1** Sensitivity of the In-BC density to variations in the number fraction of nearly hydrophobic (NH) POA (a), the hygroscopic parameter of SOA (b), the POA density (c), the SOA density (d), the externally mixed BC density (e) and the harmonic mean of multiple factors (f).

The uncertainty analysis shows that, by comparing the results based on the mean fractions of the $NF_{NH\text{-}POA}$ with a typical atmospheric observed range of 50-90 % for the $NF_{NH\text{-}POA}$ (Liu et al., 2021a), we show that the assumption on $NF_{NH\text{-}POA}$ can lead to relative deviations (uncertainty) of -17 %–+27 % for the retrieved BC density (Fig.3a).

In addition, unlike inorganics (eg., $NH_4HSO_4$, $(NH_4)_2SO_4$ and $NH_4NO_3$), which the hygroscopicity has been already well-understood (Petters and Kreidenweis, 2007), the hygroscopicity of organic species varies largely due to the complexity in organic aerosol constituents. Therefore, the assumption of the values of $\kappa_{SOA}$ will add the uncertainty in the calculation of BC density. Previous studies have suggested that the organics has a wide range of $\kappa$ values ranging from 0.05 to 0.3 (Jimenez et al., 2009; Mei et al., 2013). Thus, the sensitivity test has also been done to examine the effect due to changes in $\kappa_{SOA}$ on calculating the density of BC (Fig. 1a). The result shows that the assumption of $\kappa_{SOA}$ value can cause an average relative deviation of -10 %–+3 % in calculating the density of In-BC (Fig. 3b).

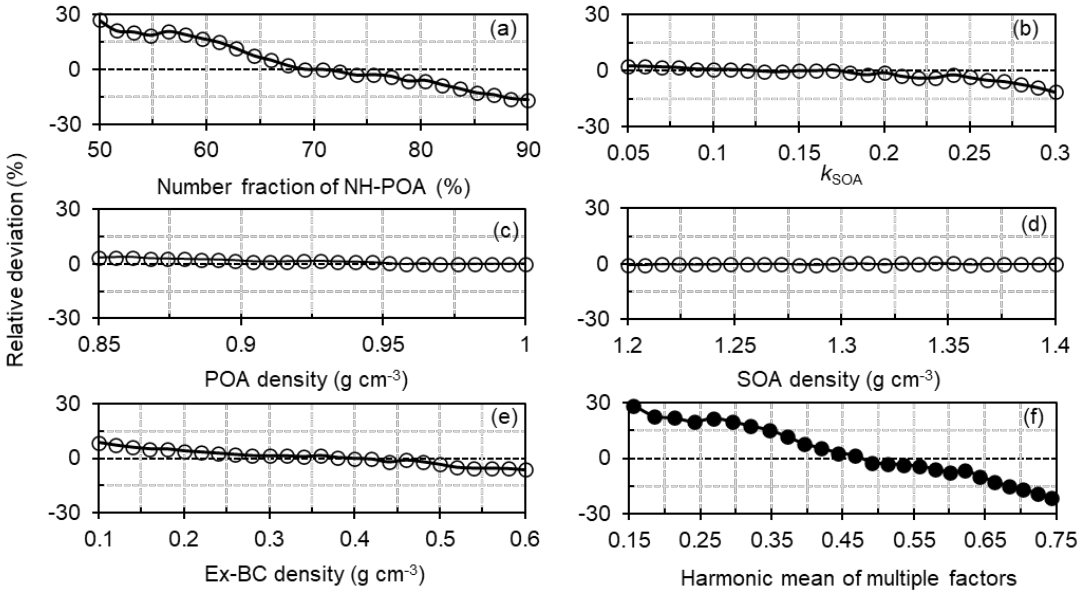


**Fig. R2** Relative deviations of the number fraction of nearly hydrophobic (NH) POA to the In-BC density (a), the hygroscopic parameter of OA to the In-BC density (b), the POA density to the In-BC density (c), the SOA density to the In-BC density (d), the externally mixed BC density to In-BC density (e) and the combined deviations based on multiple factors mentioned above (f).

However, the sensitivity test shows that the impact of both the $\rho_{POA}$ and $\rho_{SOA}$ variations on the BC density estimation is very small or even negligible (Fig. 1b, c). By varying the $\rho_{POA}$ from 0.85 to 1.0 g cm$^{-3}$ and the $\rho_{SOA}$ from 1.2 to 1.4 g cm$^{-3}$ according to the literatures (Noureddini et al., 1992; Alfarra et al., 2006; Reyes-Villegas et al., 2018), the retrieval uncertainties in the BC density are within $\pm 5$ % and $\pm 1$ % respectively (Fig. 3c, d). For $\rho_{Ex\text{-}BC}$, it exhibits that the evolution of the $\rho_{Ex\text{-}BC}$ could lead to an average deviation of $\pm 10$ % in calculating In-BC density (Fig. 3e) when increasing the values of $\rho_{Ex\text{-}BC}$ from 0.1 to 0.6 g cm$^{-3}$, which represents a typical range in ambient atmosphere (Wu et al., 2019; Liu et al., 2020). A combined uncertainty ($\delta$) caused by the multiple factors ($\delta_i$), which is calculated by equation 12, is -21 %–+29 % as shown in Fig. 3f.

$$\delta = \sqrt{\sum_{i=1}^{n} {\delta_i}^2} \qquad (12)”$$

The authors attribute the density fluctuations of the internally mixed BC and the bulk BC to the mixing state and the rapid aging from the variation of emissions (Fig. 3b&c). However, how the changes of emissions affect the parameters contributing to the density remains unexplored. For example, how the parameters in equation 8 are affected

by changing the emissions? In addition, it is difficult to discriminate the in-BC and ex-BC in Fig. 3a. It is suggested to change the color of the in-BC to increase the contrast between them.

Re: It is a good point to include some discussions about how the changes of emissions affect the parameters contributing to the density. In equation 9 for the revised text, as the reviewer commented, the assumptions on the parameters, e.g. $k_{SOA,}$ $\rho_{POA}$, can cause errors or bias to the retrieved value of BC density because of the changes in emissions and atmospheric processes of the particles. For example, the aging process may change the number fraction of the nearly-hydrophobic POA particles. Here, the observed fraction of bare POA from the total POA particles (bare POA and POA-containing) from the contemporaneous observations in literature (Liu et al., 2021a) was referred. Also, the variations of $\rho_{Ex\text{-}BC}$ have been demonstrated from the diesel exhaust (Park et al., 2003) to urban environments (Rissler et al., 2014; Wu et al., 2019). Additionally, the density of POA, SOA and the hygroscopic parameter of SOA ($k_{SOA}$) may also vary in different environments due to the changes in emissions or atmospheric aging processes of particles. For example, Wu et al. (2016) showed that the POA density was like the value of lubricating oil (1.0 g $cm^{-3}$). As the cooking organic aerosols represent a high contribution to POA in urban environments, the POA density might decrease. Thus, we investigated the sensitivity of variations of $\rho_{POA}$ to the BC density by ranging the $\rho_{POA}$ from 0.85 to 1.0 g $cm^{-3}$ according to the literatures (Noureddini et al., 1992; Alfarra et al., 2006; Reyes-Villegas et al., 2018). Similarly, the SOA density may differ due to their precursors and the formation mechanism. For example, the effective density for the 1,3,5-trimethylbenzene SOA ranged from 1.35–1.40 g $cm^{-3}$, while that for α-pinene SOA ranged from 1.29–1.32 g $cm^{-3}$ (Alfarra et al., 2006). The hygroscopicity of OA varies largely depending on the chemical composition, types, and emissions of gas precursors under different environmental conditions (Fan et al., 2020; Zhang et al., 2015), with a wide range of $\kappa$ values from 0.05 to 0.3 (Jimenez et al., 2009; Mei et al., 2013).

For these reasons, we have investigated the sensitivities of In-BC density to the variations of the assumptions on the parameters in **Section 2.3 (Lines 316-346, Fig. R2)** or as follows:

"… The uncertainty analysis shows that, by comparing the results based on the mean fractions of the $NF_{NH\text{-}POA}$ with a typical atmospheric observed range of 50-90 % for the $NF_{NH\text{-}POA}$ (Liu et al., 2021a), we show that the assumption on $NF_{NH\text{-}POA}$ can lead

to relative deviations (uncertainty) of -17 %–+27 % for the retrieved BC density (Fig.3a).

In addition, unlike inorganics (eg., $NH_4HSO_4$, $(NH_4)_2SO_4$ and $NH_4NO_3$), which the hygroscopicity has been already well-understood (Petters and Kreidenweis, 2007), the hygroscopicity of organic species varies largely due to the complexity in organic aerosol constituents. Therefore, the assumption of the values of $\kappa_{SOA}$ will add the uncertainty in the calculation of BC density. Previous studies have suggested that the organics has a wide range of $\kappa$ values ranging from 0.05 to 0.3 (Jimenez et al., 2009; Mei et al., 2013). Thus, the sensitivity test has also been done to examine the effect due to changes in $\kappa_{SOA}$ on calculating the density of BC (Fig. 1a). The result shows that the assumption of $\kappa_{SOA}$ value can cause an average relative deviation of -10 %–+3 % in calculating the density of In-BC (Fig. 3b).

However, the sensitivity test shows that the impact of both the $\rho_{POA}$ and $\rho_{SOA}$ variations on the BC density estimation is very small or even negligible (Fig. 1b, c). By varying the $\rho_{POA}$ from 0.85 to 1.0 g $cm^{-3}$ and the $\rho_{SOA}$ from 1.2 to 1.4 g $cm^{-3}$ according to the literatures (Noureddini et al., 1992; Alfarra et al., 2006; Reyes-Villegas et al., 2018), the retrieval uncertainties in the BC density are within $\pm 5$ % and $\pm 1$ % respectively (Fig. 3c, d). For $\rho_{Ex\text{-}BC}$, it exhibits that the evolution of the $\rho_{Ex\text{-}BC}$ could lead to an average deviation of $\pm 10$ % in calculating In-BC density (Fig. 3e) when increasing the values of $\rho_{Ex\text{-}BC}$ from 0.1 to 0.6 g $cm^{-3}$, which represents a typical range in ambient atmosphere (Wu et al., 2019; Liu et al., 2020). A combined uncertainty ($\delta$) caused by the multiple factors ($\delta_i$), which is calculated by equation 12, is -21 %–+29 % as shown in Fig. 3f …”

(2) According to the reviewer's suggestion, the color of the Fig 3a has been adjusted (**Fig. R3** or **Fig. 4**) as follows,

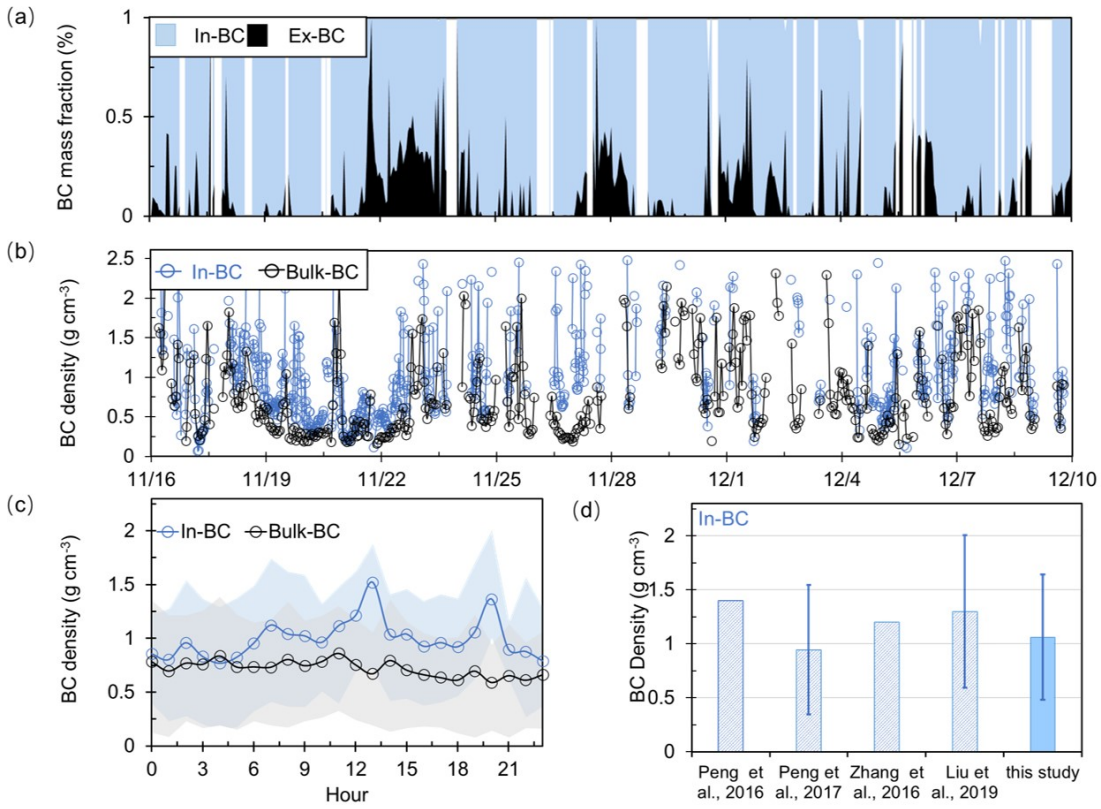


**Fig. R3** (a) Time series of the mass fraction of the retrieved internal- and external-mixed BC; (b) Time series of the retrieved density of the bulk and internal- mixed BC (In-BC); (c) Diurnal variation of the retrieved density of bulk and In-BC; (d) Comparison of the results of the derived In-BC density in this study with that reported in literatures.

Pertinent to comment #2, what factors determine the retrieved BC density? Are they explicit in equation 8? How the correlations between those factors and the BC density? Can the authors explore more on this?

Re: Thanks for the comments. For the retrieval, the assumptions on the values of $\kappa_{SOA}$, $\rho_{POA}$, $\rho_{SOA}$ and $\rho_{Ex\text{-}BC}$ as well as the fraction of primary organic aerosols in non-hygroscopic or hygroscopic mode would add uncertainty in the inferred values of ambient internally-mixed BC density. To investigate the main factors determining the retrieved BC density, we evaluate the sensitivities of In-BC density to the variations of these factors in Section **2.3**. The results suggest that the number fraction of non-hygroscopic POA ($NF_{NH\text{-}POA}$) and the hygroscopic parameter of SOA have larger

impacts on the estimation of BC density compared to other factors. The correlations between $NF_{\text{NH-POA}}$, $\kappa_{\text{SOA}}$, $\rho_{\text{POA}}$, $\rho_{\text{SOA}}$ as well as $\rho_{\text{Ex-BC}}$ and the In-BC density are quantified as shown in **Fig. R1** or Fig. 2.

Some discussions about this have been included in the revised paper, see **Lines 298-306**, as follows:

"…The figures show that the In-BC density gradually decreases with the increment of the $NF_{\text{NH-POA}}$, implying the higher fraction of bare POA particles correspond to the early aging stage of aerosol particles. With increase of $\kappa_{\text{SOA}}$, the In-BC density is generally reduced, but with small fluctuations (Fig.1a, Fig. 2b). This suggests a complex impact of assumptions of $\kappa_{\text{SOA}}$ on the retrieved BC density. In addition, the In-BC density decreases very slightly as $\rho_{\text{Ex-BC}}$ increases (Fig. 2e), suggesting applying a larger $\rho_{\text{Ex-BC}}$ would derive smaller values for In-BC density. The In-BC density is insensitive to the changes of the density of POA and SOA, showing an almost negligible effect on the retrieved results (Fig. 2c and d) …"

The calculation of critical size is based on pure water assumption for the surface tension and water density, which may cause uncertainties. The authors should discuss the uncertainties associated with the assumption.

Re: It is true that there may be some uncertainties by assuming the surface tension (σ) and water density in calculating the critical diameter. The organic matter in particles can act as surfactants to lower the surface tension of the particles and hence increase the CCN activity (Ovadnevaite et al., 2017). The effect of the surface tension on CCN activity have been explored in both filed and laboratory studies (McFiggans et al., 2006; Meng et al., 2014; Ovadnevaite et al., 2017; Cai et al., 2018; Hu et al., 2020). For example, Ovadnevaite et al. (2017) found that a reduction of σ from 0.072 to 0.049 J $m^{-2}$ was required to meet with the CCN measurement for the higher supersaturations (SS). Cai et al. (2018) also suggested that the CCN number concentration would be undepreciated if the surface tension of pure water was used. Meng et al. (2014) showed that the surface tension depression may be more pronounced at small particle sizes, which is because the organics are more concentrated on small particles. These results suggest that the usage of the surface tension of pure water would overestimate the critical diameter and underpredict CCN number concentration but more pronounced at small particle sizes. In our study, the SS for CCN activity was set to 0.23 % and 0.40 %, which represent the common supersaturation conditions for stratiform or moderately convective clouds (Moteki et al., 2019), with larger critical diameters of about 90 nm

and 70 nm. Some discussions about their effect on the critical diameter and CCN number concentration have been included in the revised paper, see **Lines 459-469**, as follows:

"… It should be noted that the assumption of the surface tension of water would overestimate the critical diameter and underpredict CCN number concentration. While the surface tension depression might be more obvious for the small size particles (<60 nm), as the fraction of organics are higher at small particles size (Meng et al., 2014; Cai et al., 2018). Here, in this study, we calculated the critical diameters at supersaturations of 0.40 % and 0.23 %, typical values in cloud, corresponding to larger sizes (> 70 nm and 90 nm) of aerosols. Therefore, the uncertainties from the application of the surface tension of pure water should be negligible (< 10 %). Here, three schemes were assumed to evaluate the effect of BC density and mixing state on prediction of CCN number concentrations. The detailed calculation methods are presented in the supporting information (SI: Methods) or referenced from Ren et al., 2018 …"

In addition, the density of water would change with temperature, which might bring some bias in calculating the critical size. Here, in our study, to make the results comparable, all the parameters were adjusted to standard conditions in the $\kappa$-Köhler relationship (eg., temperature, density water) (Petters & Kreidenweis, 2007). Some introductions about the uncertainty of water density have been added in the **supplement**, or as follow:

"… By applying the hygroscopicity parameter $\kappa_{chem}$ into $\kappa$-Köhler relationship (Petters & Kreidenweis, 2007), the critical diameter or activation diameter ($D_{cut}$) can be obtained at a given supersaturation ($S$). Thus, the CCN concentration can be predicted by using the critical diameter and particle number size distribution.

The equations used in the estimating $N_{CCN}$ are as follows,

$$CCN_{pre} = \int_{D_{cut}}^{D_{end}} n(log\ D_p) d\ log\ D_p \quad (1)$$

where $D_{cut}$ is the critical diameter, $D_{end}$ is the upper size limit of the particle number size distribution (PNSD), $n$ (log $D_p$) is the function of the aerosol number size distribution.

$$D_{cut} = \sqrt[3]{\frac{4A^3}{27\kappa ln^2 S}}, \qquad A = \frac{4\sigma_{s/a} M_w}{RT\rho_w} \quad (2)$$

where $\kappa$ is the hygroscopicity parameter, $S$ is a given supersaturation, $M_w$ is the molecular weight of water, $\sigma_{s/a}$ is the surface tension of pure water, $\rho_w$ is the density of water, $R$ is the gas constant, and $T$ is the absolute temperature. Here the parameters $T$ and $\rho_w$ were adjusted to standard conditions ($T$=298.15K) ..."

In Fig. 5, what is the measured Nccn. What method is this based on? Are they the same for the Nccn in Fig. 5 and Fig. 6? How are the differences between the CCN number concentration predicted based on the retrieved BC density and based on the HTDMA? Can the authors discuss more on this?

Re: The $N_{CCN}$ in Fig. 5 was measured by a Droplet Measurement Technologies CCN counter (CCNc, DMT; Lance et al., 2006), which is widely used in the measurement of CCN number concentration. During the field campaigns, atmospheric particles were sampled after a $PM_{2.5}$ impactor and then dried by a Nafion tube before being measured by instrument. The relative humidity of the sample flow was below 30 %. Polydisperse dry aerosol was neutralized with a Kr-85 diffusion charger and introduced into a differential mobility analyzer (DMA, TSI 3081) to output mono-dispersed particle. The mono-dispersed aerosol is then split between a condensation particle counter (CPC, TSI 3772) with flow rate of 0.5 L $min^{-1}$ and a Cloud Condensation Nucleus counter (CCNc, DMT) with flow rate of 0.5 L $min^{-1}$. At each particle dry size, the CCN number concentration measured by the CCNc can be obtained, hereby the $N_{CCN}$ was obtained by integrating over the size range. Detailed description about the instrument and data correction can be found in Ren et al., 2018 and here a brief introduction was given in this study. The measured $N_{CCN}$ in Fig. 5 and Fig. 6 are same.

Therefore, in this study, the effect of BC density on CCN activity was investigated through the CCN closure of the measured $N_{CCN}$ and the precited $N_{CCN}$. The measured $N_{CCN}$ is based on the measurement of CCN counter, not HTDMA. The precited $N_{CCN}$ is calculated by using the critical diameter and the particle number size distribution. The critical diameter is calculated based on Köhler theory and ZSR rule. For a multicomponent particle, the Zdanovskii–Stokes– Robinson (ZSR) mixing rule (Stokes and Robinson, 1966) can also estimate $\kappa_{chem}$ using chemical composition data:

$$\kappa_{chem} = \sum_i \varepsilon_i \kappa_i \quad (1)$$

where $\varepsilon_i$ and $\kappa_i$ are the volume fraction and $\kappa$ for the $i$th chemical component, respectively.

The BC density was retrieved based on the closure between the $\kappa_{gf}$ from HTDMA and $\kappa_{chem}$. The $\kappa_{gf}$ is derived using $\kappa$-Köhler theory based on hygroscopic growth factor (Gf) (Petters and Kreidenweis, 2007). The $\kappa_{chem}$ is calculated based on chemical volume fractions by using the ZSR rule according to the equation 1.

Minor comments: there are a lot of typos, ill-sentences which need to be cleared in the revised version.

- Title: I am not quite sure this is a new method

  Re: Previously, the BC density are usually directly measured by several techniques, such as an integrated system of a volatility tandem differential mobility analyzer and a single particle soot photometer (VTDMA-SP2) (Zhang et al., 2016), or a differential mobility analyzer with a SP2 (DMA-SP2) (Olfert et al., 2007; Rissler et al., 2014; Wu et al., 2019), and a differential mobility analyzer–centrifugal particle analyzer–single-particle soot photometer (DMA–CPMA–SP2) system (Liu et al., 2019b; Yu et al., 2020), etc. To our knowledge, this is, for the first time, we derived the BC density by using the by combining field measured hygroscopic growth factor and aerosol chemical composition and Köhler theory. Therefore, we think it is a new method.

- L40-41, such an effect

  Re: The sentence has been revised "We also find that the $N_{CCN}$ is more sensitive to the variations of BC density when it is <1.0 g $cm^{-3}$. This illustrates a necessity of accounting for the effect of BC density on CCN activity closer to source regions where the BC particles are mostly freshly emitted."

- L44: applying varying BC density, an awkward phrase, please change it

  Re: The phrase has been revised "applying variable BC density"

- L50: The light-absorbing capability

  Re: Revised.

- L57: well understood

  Re: Revised.

- L61 and others: While after aging, this is strange since it is just one sentence. There are some more the same issues throughout the manuscript.

  Re: The sentence has been revised as "When the BC particles were emitted, they generally mix with other materials by condensation, coagulation, and other processes (Riemer et al., 2004; Zhang et al., 2008; Liu et al., 2013; Zhang et al., 2020a) ..." The other sentences throughout the manuscript with the same issues have been revised (see the revised text).

- L63: The BC structure.

  Re: Revised.

- L71: the average BC density

  Re: Revised.

- L74: than that internal/ aged BC …, seems a broken sentence

  Re: The sentence has been revised as “Field measurements have also indicated that a considerable fraction of externally mixed/uncoated BC exists (Clarke et al., 2004; Cheng et al., 2012;), although a higher proportion of internally mixed/aged BC particles in the ambient atmosphere were observed (Schwarz et al., 2008; Massoli et al., 2015; Chen et al., 2020).”
- L76: internally doesn’t need a hyphen after the word

  Re: Revised.
- L78: climate effect

  Re: Revised.
- L81: particle hygroscopicity

  Re: Revised.
- L85: was found caused by?

  Re: The sentence has been revised as “In addition, when estimating the CCN number concentration, a significant bias of –35 % ~ +20 % was found due to the assumption of particle mixing state (Ren et al., 2018).”
- L87: yet accounted for

  Re: Revised.
- L94: reference cited, format is not consistent

  Re: Revised.
- L116: change “Then” to “Subsequently”

  Re: Revised.
- L120: Here, four diameters

  Re: Revised.
- L126: by using, “by” should be deleted. Please check throughout the manuscript

  Re: Thanks a lot. Revised.
- L128: et al., 2009. I am not sure this can be cited like this way. Please check throughout the manuscript

  Re: Revised.
- L141, where Gf is …. This still belongs to the above paragraph, why it needs to be dented? Check all the occasions.

  Re: Revised.
- L157-158: assumed mixed with the other?

Re: The method of retrieving the mixing state of BC has been revised. “Since the number fraction of the nearly-hydrophobic POA would change with the emission and aging processes, in this study, we have applied different values for the number fractions of hydrophobic POA (NH-POA) under clean (91 %), moderately polluted (70 %), and heavily polluted conditions (31 %) by referring the literature (Liu et al., 2021a), as shown in Fig. S2.”

- L158: And thus to “Thus”
  Re: Revised.
- L160: externally mixed
  Re: Revised.
- L174: mass size distributions was modeled as?
  Re: The sentence has been revised as “The mass size distribution of Ex-BC was fit using the log-normal distribution as shown in Fig. S4 (Wu et al., 2017; Liu et al., 2019a; Zhao et al., 2022).”
- L182: by minus? by subtracting
  Re: Revised.
- L188: is with an assumption of to assumes
  Re: Revised.
- L193-194: which showed an independence on particle size when the Dp >100 nm during the campaign period (Fan et al., 2020), was averaged and applied for the retrieval. It is hard to understand what this sentence means
  Re: The sentence has been revised as “Second, since the size distribution of BC number concentration is usually with peaks between 100 and 200 nm (Liu et al., 2019a; Yu et al., 2020; Zhao et al., 2022), the $\kappa_{gf\text{-}MH}$ value of particles in accumulation mode was averaged and applied for the retrieval. Previous studies showed an independence of $\kappa_{gf\text{-}MH}$ on particle size when the $D_p$ >100 nm during the campaign period (Fan et al., 2020). Therefore, the average of $\kappa_{gf\text{-}MH}$ in accumulation mode is reasonable for the determination of the In-BC density.”
- L209: in equation (7), no article “the”. Check all occasions
  Re: Revised.
- L219-220: were taken from previous studies
  Re: Revised.
- L221-222: assumed to be
  Re: Revised.

- L222: The values of … was?

  Re: The sentence has been revised as "The values of $\kappa$ for inorganic components are 0.56 for $NH_4HSO_4$, 0.48 for $(NH_4)_2SO_4$ and 0.58 for $NH_4NO_3$, along with the best-fit values for the three inorganic salts (Petters & Kreidenweis, 2007 and Gunthe et al., 2009)."
- L235: unlike inorganics, which the hygroscopicity, what is "which" referred to?

  Re: Here "which" is referred to the inorganics, such as $NH_4HSO_4$, $(NH_4)_2SO_4$ and $NH_4NO_3$. The sentence has been revised as "In addition, unlike inorganics (eg., $NH_4HSO_4$, $(NH_4)_2SO_4$ and $NH_4NO_3$), which the hygroscopicity has been already well-understood (Petters and Kreidenweis, 2007), the hygroscopicity of organic species varies largely due to the complexity in organic aerosol constituents."
- L272: for calculating the …

  Re: Revised.
- L273: with the assumption of to assuming

  Re: Revised.
- L278: internally and externally mixed

  Re: Revised.
- L280: the atmospheric aging process

  Re: Revised.
- L287: with both those?

  Re: Revised.
- L289/303/315: internally mixed

  Re: Revised.
- L305: The density of the In-BC during daytime was

  Re: Revised.
- L309: The slight decreases

  Re: Revised.
- L313: The diurnal cycles in BC density are consistent with those measured

  Re: Revised.
- L322: McMurry

  Re: Revised.
- L330: Mean probability distribution function (PDF) of the density of bulk and In-BC retrieved by this study is

  Re: Revised.

- L332: with a peak value

  Re: Revised.
- L333: externally mixed and internally mixed

  Re: Revised.
- L338: typical internal mixed BC

  Re: Revised.
- L341: A previous study showed that the use of an inaccurate density value of …

  Re: The sentence has been revised as "A previous study showed that the use of an inaccurate density value of BC particles would result in large bias in estimating $\kappa$ of ambient aerosol particles with the ZSR mixing rule (Fan et al., 2020), as would further lead to uncertainties in prediction of $N_{CCN}$ and relevant climate effects."
- L345: what "it" represents here?

  Re: "it" represents the BC particles.
- L350: on predicted CCN number concentrations

  Re: Revised.
- L360: in the atmosphere),

  Re: Revised.
- Section 3.3, use 0.23% instead of 0.2%

  Re: The SS levels, eg., 0.20 % and 0.40 % were set in the CCNc instrument. The operation SS of CCNc was calibrated using pure ammonium sulfate particles following Rose et al. (2008). The corrected SS levels were 0.23 % and 0.40 %. The SS level of 0.20 % has been revised to 0.23 %.
- L414: would cause

  Re: Revised.
- L417-418: by assumption of to assuming

  Re: Revised.
- L435: the current assumption

  Re: Revised.

**References:**

Ivleva, N. P., Messerer, A., Yang, X., Niessner, R., and Poschl, U.: ¨ Raman microspectroscopic analysis of changes in the chemical structure and reactitivity of soot in a diesel exhaust aftertreatment model system, Environ. Sci. Technol., 41, 3702–3707, 2007.

Peng, J. F., Hu, M., Guo, S., Du, Z. F., Zheng, J., Shang, D. J., Zamora, M., Zeng, L. M., Shao, M., Wu, Y. S., Zheng, J., Wang, Y., Glen, C., Collins, D., Molina, M., and Zhang, R. Y.: Markedly enhanced absorption, and direct radiative forcing of black carbon under polluted urban

environments, P. Natl. Acad. Sci. USA, 113(16), 4266–4271, https://doi.org/10.1073/pnas.1602310113, 2016.

Bond, T. C., Doherty, S. J., Fahey, D., Forster, P., Berntsen, T., DeAngelo, B., Flanner, M., Ghan, S., Kärcher, B., and Koch, D.: Bounding the role of black carbon in the climate system: A scientific assessment, J. Geophys. Res.-Atmos., 118(11), 5380–5552, https://doi.org/10.1002/jgrd.50171, 2013

Dameto de España, C., Wonaschütz, A., Steiner, G., Rosati, B., Demattio, A., Schuh, H., and Hitzenberger, R.: Long-term quantitative field study of New Particle Formation (NPF) events as a source of Cloud Condensation Nuclei (CCN) in the urban background of Vienna, Atmos. Environ., 164, 289–298, https://doi.org/10.1016/j.atmosenv.2017.06.001, 2017.

Li, M., Zhang, Q., Kurokawa, J.-I., Woo, J.-H., He, K., Lu, Z., Ohara, T., Song, Y., Streets, D. G., Carmichael, G. R., Cheng, Y., Hong, C., Huo, H., Jiang, X., Kang, S., Liu, F., Su, H., and Zheng, B.: MIX: a mosaic Asian anthropogenic emission inventory under the international collaboration framework of the MICS-Asia and HTAP, Atmos. Chem. Phys., 17, 935–963, https://doi.org/10.5194/acp-17-935-2017, 2017.

Liu, D., Joshi, R., Wang, J., Yu, C., Allan, J. D., Coe, H., Flynn, M. J., Xie, C., Lee, J., Squires, F., Kotthaus, S., Grimmond, S., Ge, X., Sun, Y., and Fu, P.: Contrasting physical properties of black carbon in urban Beijing between winter and summer, Atmos. Chem. Phys., 19, 6749–6769, https://doi.org/10.5194/acp-19-6749-2019, 2019a.

Riemer, N., Vogel, H., and Vogel, B.: Soot aging time scales in polluted regions during day and night, Atmos. Chem. Phys., 4, 1885–1893, https://doi.org/10.5194/acp-4-1885-2004, 2004.

Zhang, R. Y., Khalizov, A. F., Pagels, J., Zhang, D., Xue, H. X., and McMurry, P. H.: Variability in morphology, hygroscopicity, and optical properties of soot aerosols during atmospheric processing, P. Natl. Acad. Sci. USA, 105, 10291–10296, https://doi.org/10.1073/pnas.0804860105, 2008.

Liu, D., Allan, J., Whitehead, J., Young, D., Flynn, M., Coe, H., McFiggans, G., Fleming, Z. L., and Bandy, B.: Ambient black carbon particle hygroscopic properties controlled by mixing state and composition, Atmos. Chem. Phys., 13, 2015–2029, https://doi.org/10.5194/acp-13-2015-2013, 2013.

Zhang, F., Wang, Y., Peng, J., Chen, L., Sun, Y., Duan, L., Ge, X., Li, Y., Zhao, J., Liu, C., Zhang, X., Zhang, G., Pan, Y., Wang, Y., Zhang, A. L., Ji, Y., Wang, G., Hu, M., Molina, M. J., Zhang, R.: An unexpected catalyst dominates formation and radiative forcing of regional haze, P. Natl. Acad. Sci. USA, 117(8), 3960-3966, https://doi.org/10.1073/pnas.1919343117, 2020a.

Cheng, Y. F., Eichler, H., Wiedensohler, A., Heintzenberg, J., Zhang, Y. H., Hu, M., Herrmann, H., Zeng, L. M., Liu, S., Gnauk, T., Brüggemann, E., and He, L. Y.: Mixing state of elemental carbon and non-light-absorbing aerosol components derived from in situ particle optical properties at Xinken in Pearl River Delta of China, J. Geophys. Res., 111, D20204, doi:10.1029/2005JD006929, 2006.

Zhang, Y., Zhang, Q., Cheng, Y., Su, H., Kecorius, S., Wang, Z., Wu, Z., Hu, M., Zhu, T., Wiedensohler, A., and He, K.: Measuring the morphology and density of internally mixed black carbon with SP2 and VTDMA: new insight into the absorption enhancement of black carbon in the atmosphere, Atmos. Meas. Tech., 9, 1833–1843, https://doi.org/10.5194/amt-9-1833-2016, 2016.

Peng, J. F., Hu, M., Guo, S., Du, Z. F., Zheng, J., M., Zeng, L. M., Shao, M., Wu, Y. S., Collins, D., Molina, M., and Zhang, R. Y.: Ageing and hygroscopicity variation of black carbon particles in Beijing measured by a quasi-atmospheric aerosol evolution study (QUALITY) chamber, Atmos.

Chem. Phys., 17(17), 10333-10348, https://doi.org/10.5194/acp-17-10333-2017, 2017.

Wu, Y., Wang, X., Tao, J., Huang, R., Tian, P., Cao, J., Zhang, L., Ho, K.-F., Han, Z., and Zhang, R.: Size distribution and source of black carbon aerosol in urban Beijing during winter haze episodes, Atmos. Chem. Phys., 17, 7965–7975, https://doi.org/10.5194/acp-17-7965-2017, 2017.

Liu, D., Joshi, R., Wang, J., Yu, C., Allan, J. D., Coe, H., Flynn, M. J., Xie, C., Lee, J., Squires, F., Kotthaus, S., Grimmond, S., Ge, X., Sun, Y., and Fu, P.: Contrasting physical properties of black carbon in urban Beijing between winter and summer, Atmos. Chem. Phys., 19, 6749–6769, https://doi.org/10.5194/acp-19-6749-2019, 2019a.

Zhao, G., Tan, T., Hu, S., Du, Z., Shang, D., Wu, Z., Guo, S., Zheng, J., Zhu, W., Li, M., Zeng, L., and Hu, M.: Mixing state of black carbon at different atmospheres in north and southwest China, Atmos. Chem. Phys., 22, 10861–10873, https://doi.org/10.5194/acp-22-10861-2022, 2022.

Rader, D.J., McMurry, P.H.: Application of the tandem differential mobility analyzer to studies of droplet growth or evaporation, J. Geophys. Res.- Atmos., 17, 771-787, https://doi.org/10.1016/0021-8502(86)90031-5, 1986.

Geller, M., Biswas, S., and Sioutas, C.: Determination of particle effective density in urban environments with a differential mobility analyzer and aerosol particle mass analyzer, Aerosol Sci. Technol., 40, 709–723, https://doi.org/10.1080/02786820600803925, 2006.

Wu, Y. F., Xia, Y. J., Huang, R. J., Deng, Z. Z., Tian, P., Xia, X. G., et al.: A study of the morphology and effective density of externally mixed black carbon aerosols in ambient air using a size-resolved single-particle soot photometer (SP2), Atmos. Meas. Tech., 12, 4347–4359, https://doi.org/10.5194/amt-12-4347-2019, 2019.

Liu, H., Pan, X., Liu, D., Liu, X., Chen, X., Tian, Y., Sun, Y., Fu, P., and Wang, Z.: Mixing characteristics of refractory black carbon aerosols at an urban site in Beijing, Atmos. Chem. Phys., 20, 5771–5785, https://doi.org/10.5194/acp-20-5771-2020, 2020.

Stokes, R. and Robinson, R.: Interactions in aqueous nonelectrolyte solutions, I. Solute-solvent equilibria, J. Phys. Chem.-US, 70, 2126–2131, 1966.

Petters, M. D. and Kreidenweis, S. M.: A single parameter representation of hygroscopic growth and cloud condensation nucleus activity, Atmos. Chem. Phys., 7, 1961–1971, https://doi.org/10.5194/acp-7-1961-2007, 2007.

Yu, C., Liu, D., Broda, K., Joshi, R., Olfert, J., Sun, Y., Fu, P., Coe, H., Allan, J.D.: Characterising mass-resolved mixing state of black carbon in Beijing using a morphology-independent measurement method, Atmos. Chem. Phys., 20, 3645–3661. https://doi.org/10.5194/acp-20-3645-2020, 2020.

Fan, X., Liu, J., Zhang, F., Chen, L., Conllins, D., Xu, W., Jin, X., Ren, J., Wang, Y.,Wu, H., Li, S., Sun, Y., Li, Z.: Contrasting size-resolved hygroscopicity of fine particles derived by HTDMA and HR-ToF-AMS measurements between summer and winter in Beijing: the impacts of aerosol aging and local emissions, Atmos. Chem. Phys. 20, 915-929, https://doi.org/10.5194/acp-20-915-2020, 2020.

Stokes, R. and Robinson, R.: Interactions in aqueous nonelectrolyte solutions, I. Solute-solvent equilibria, J. Phys. Chem.-US, 70, 2126–2131, 1966.

Gysel, M., Crosier, J., Topping, D. O., Whitehead, J. D., Bower, K. N., Cubison, M. J., Williams, P. I., Flynn, M. J., McFiggans, G. B., and Coe, H.: Closure study between chemical composition and hygroscopic growth of aerosol particles during TORCH2, Atmos. Chem. Phys., 7, 6131–6144, https://doi.org/10.5194/acp-7-6131-2007, 2007.

Wu, Z. J., Zheng, J., Shang, D. J., Du, Z. F., Wu, Y. S., Zeng, L. M., Wiedensohler, A., and Hu, M.: Particle hygroscopicity and its link to chemical composition in the urban atmosphere of Beijing, China, during summertime, Atmos. Chem. Phys., 16, 1123– 1138, https://doi.org/10.5194/acp-16-1123-2016, 2016.

Dinar, E., Mentel, T. F., and Rudich, Y.: The density of humic acids and humic like substances (HULIS) from fresh and aged wood burning and pollution aerosol particles, Atmos. Chem. Phys., 6, 5213–5224, doi:10.5194/acp-6-5213-2006, 2006.

Reyes-Villegas, E., Bannan, T., Le Breton, M., Mehra, A., Priestley, M., Percival, C., Coe, H., and Allan, J. D.: Online Chemical Characterization of Food-Cooking Organic Aerosols: Implications for Source Apportionment, Environ. Sci. Technol., 52, 5308–5318, https://doi.org/10.1021/acs.est.7b06278, 2018.

Gunthe, S. S., King, S. M., Rose, D., Chen, Q., Roldin, P., Farmer, D. K., Jimenez, J. L., Artaxo, P., Andreae, M. O., Martin, S. T., and Pöschl, U.: Cloud condensation nuclei in pristine tropical rainforest air of Amazonia: size resolved measurements and modeling of atmospheric aerosol composition and CCN activity, Atmos. Chem. Phys., 9, 7551–7575, https://doi.org/10.5194/acp-9-7551-2009, 2009.

Chang, R. Y.-W., Slowik, J. G., Shantz, N. C., Vlasenko, A., Liggio, J., Sjostedt, S. J., Leaitch, W. R., and Abbatt, J. P. D.: The hygroscopicity parameter ($\kappa$) of ambient organic aerosol at a field site subject to biogenic and anthropogenic influences: relationship to degree of aerosol oxidation, Atmos. Chem. Phys., 10, 5047–5064, https://doi:10.5194/acp-10-5047-2010, 2010.

Kawana, K., Nakayama, T., and Mochida, M.: Hygroscopicity and CCN activity of atmospheric aerosol particles and their relation to organics: Characteristics of urban aerosols in Nagoya, Japan, J. Geophys. Res.-Atmos., 121, 4100–4121, https://doi.org/10.1002/2015JD023213, 2016.

Alfarra, M. R., Paulsen, D., Gysel, M., Garforth, A. A., Dommen, J., Prévôt, A. S. H., Worsnop, D. R., Baltensperger, U., and Coe, H.: A mass spectrometric study of secondary organic aerosols formed from the photooxidation of anthropogenic and biogenic precursors in a reaction chamber, Atmos. Chem. Phys., 6, 5279– 5293, https://doi:10.5194/acp-6-5279-2006, 2006.

Zhang, R., Wang, G., Guo, S., Zamora, M. L., Ying, Q., Lin, Y.: Formation of urban fine particulate matter, Chemical Reviews, 115(10), 3803–3855, https://doi.org/10.1021/acs.chemrev.5b00067, 2015.

Liu, J., Zhang, F., Xu, W., Sun, Y., Chen, L., Li, S.: Hygroscopicity of organic aerosols linked to formation mechanisms, Geophysical Research Letters, 48, e2020GL091683, https://doi.org/10.1029/2020gl091683, 2021b.

Liu, L, Zhang, J, Zhang, Y, Wang, Y, Xu, L, Yuan, Q, et al.: Persistent residential burning-related primary organic particles during wintertime hazes in North China: insights into their aging and optical changes, Atmos. Chem. Phys. *21*, 2251–2265, https://doi.org/10.5194/acp-21-2251-2021, 2021a.

Jimenez, J. L., Canagaratna, M. R., Donahue, N. M., Prevot, A. S. H., Zhang, Q., Kroll, J. H., DeCarlo, P. F., Allan, J. D., Coe, H., Ng, N. L., Aiken, A. C., Docherty, K. S., Ulbrich, I. M., Grieshop, A. P., Robinson, A. L., Duplissy, J., Smith, J. D., Wilson, K. R., Lanz, V. A., Hueglin, C., Sun, Y. L., Tian, J., Laaksonen, A., Raatikainen, T., Rautiainen, J., Vaattovaara, P., Ehn, M., Kulmala, M., Tomlinson, J. M., Collins, D. R., Cubison, M. J., Dunlea, E. J., Huffman, J. A., Onasch, T. B., Alfarra, M. R., Williams, P. I., Bower, K., Kondo, Y., Schneider, J., Drewnick, F., Borrmann, S., Weimer, S., Demerjian, K., Salcedo, D., Cottrell, L., Griffin, R., Takami, A.,

Miyoshi, T., Hatakeyama, S., Shimono, A., Sun, J. Y., Zhang, Y. M., Dzepina, K., Kimmel, J. R., Sueper, D., Jayne, J. T., Herndon, S. C., Trimborn, A. M., Williams, L. R., Wood, E. C., Middlebrook, A. M., Kolb, C. E., Baltensperger, U., and Worsnop, D. R.: Evolution of Organic Aerosols in the Atmosphere, Science., 326, 1525–1529, https://doi.org/10.1126/science.1180353, 2009.

Mei, F., Setyan, A., Zhang, Q., and Wang, J.: CCN activity of organic aerosols observed downwind of urban emissions during CARES, Atmos. Chem. Phys., 13, 12155–12169, https://doi.org/10.5194/acp-13-12155-2013, 2013.

Noureddini, H., Teoh, B. C., Davis Clements, L.: Densities of vegetable oils and fatty acids, J. Am. Oil Chem. Soc., 69 (12), 1184−1188, 1992.

Alfarra, M. R., Paulsen, D., Gysel, M., Garforth, A. A., Dommen, J., Prévôt, A. S. H., Worsnop, D. R., Baltensperger, U., and Coe, H.: A mass spectrometric study of secondary organic aerosols formed from the photooxidation of anthropogenic and biogenic precursors in a reaction chamber, Atmos. Chem. Phys., 6, 5279– 5293, https://doi:10.5194/acp-6-5279-2006, 2006.

Rissler, J., Nordin, E. Z., Eriksson, A. C., Nilsson, P. T., Frosch, M., Sporre, M. K., Wierzbicka, A., Svenningsson, B., Londahl, J., Messing, M. E., Sjogren, S., Hemmingsen, J. G., Loft, S., Pagels, J. H., and Swietlicki, E.: Effective Density and Mixing State of Aerosol Particles in a Near-Traffic Urban Environment, Environ. Sci. Technol., 48, 6300–6308, https://doi.org/10.1021/es5000353, 2014.

Ovadnevaite, J., Zuend, A., Laaksonen, A., Sanchez, K. J., Roberts, G., Ceburnis, D., Decesari, S., Rinaldi, M., Hodas, N., Facchini, M. C., Seinfeld, J. H., and O'Dowd, C.: Surface tension prevails over solute effect in organic-influenced cloud droplet activation, Nature, 546, 637–641, 2017.

McFiggans, G., Artaxo, P., Baltensperger, U., Coe, H., Facchini, M. C., Feingold, G.: The effect of physical and chemical aerosol properties on warm cloud droplet activation, Atmospheric Chemistry and Physics, 6(9), 2593–2649, https://doi.org/10.5194/acp-6-2593- 2006, 2006.

Meng, J. W., Yeung, M. C., Li, Y. J., Lee, B. Y. L., and Chan, C. K.: Size-resolved cloud condensation nuclei (CCN) activity and closure analysis at the HKUST Supersite in Hong Kong, Atmos. Chem. Phys., 14, 10267–10282, https://doi.org/10.5194/acp-14- 10267-2014, 2014.

Cai, M., Tan, H., Chan, C. K., Qin, Y., Xu, H., Li, F., Schurman, M. I., Liu, L., and Zhao, J.: The size-resolved cloud condensation nuclei (CCN) activity and its prediction based on aerosol hygroscopicity and composition in the Pearl Delta River (PRD) region during wintertime 2014, Atmos. Chem. Phys., 18, 16419–16437, https://doi.org/10.5194/acp-18-16419-2018, 2018.

Hu, D., Liu, D., Zhao, D., Yu, C., Liu, Q., & Tian, P.: Closure investigation on cloud condensation nuclei ability of processed anthropogenic aerosols, Journal of Geophysical Research: Atmospheres, 125, e2020JD032680, https://doi.org/ 10.1029/2020JD032680, 2020.

Moteki, N., Mori, T., Matsui, H., & Ohata, S.: Observational constraint of in-cloud supersaturation for simulations of aerosol rainout in atmospheric models, Npj Climate and Atmospheric Science, 2(1), 6, https://doi.org/10.1038/s41612-019-0063-y, 2019.

Ren, J., Zhang, F., Wang, Y., Collins, D., Fan, X., Jin, X., et al.: Using different assumptions of aerosol mixing state and chemical composition to predict CCN concentrations based on field measurements in urban Beijing, Atmos. Chem. Phys., 18, 6907–6921, https://doi.org/10.5194/acp-18-6907-2018, 2018.

Lance, S., Medina, J., Smith, J., and Nenes, A.: Mapping the operation of the DMT continuous flow CCN counter, Aerosol Sci. Tech., 40, 242–254, 2006.

Clarke, A.D., Shinozuka, Y., Kapustin, V.N., Howell, S., Huebert, B., Doherty, S., Anderson, T., Covert, D., Anderson, J., Hua, X., Moore II, K.G., McNaughton, C., Carmichael, G., Weber, R.: Size distributions and mixtures of dust and black carbon aerosol in Asian outflow: physiochemistry and optical properties, J. Geophys. Res.- Atmos., 109, D15S09, https://doi.org/10.1029/2003JD004378, 2004.

Cheng, Y. F., Su, H., Rose, D., Gunthe, S. S., Berghof, M., Wehner, B., Achtert, P., Nowak, A., Takegawa, N., Kondo, Y., Shiraiwa, M., Gong, Y. G., Shao, M., Hu, M., Zhu, T., Zhang, Y. H., Carmichael, G. R., Wiedensohler, A., Andreae, M. O., and Pöschl, U.: Size-resolved measurement of the mixing state of soot in the megacity Beijing, China: diurnal cycle, aging and parameterization, Atmos. Chem. Phys., 12, 4477–4491, doi:10.5194/acp-12-4477-2012, 2012.

Chen, L., F. Zhang, P. Yan, X. Wang, L. Sun, Y. Li, X. Zhang, Y. Sun, and Z. Li.: The large proportion of black carbon (BC)-containing aerosols in the urban atmosphere, Environ. Pollut., 263, 114507, https://doi.org/10.1016/j.envpol.2020.114507, 2020.

Schwarz, J. P., Gao, R. S., Spackman, J. R., Watts, L. A., Thomson, D. S., Fahey, D. W., Ryerson, T. B., Peischl, J., Holloway, J. S., Trainer, M., Frost, G. J., Baynard, T., Lack, D. A., de Gouw, J. A., Warneke, C., and Del Negro, L. A.: Measurement of the mixing state, mass, and optical size of individual black carbon particles in urban and biomass burning emissions, Geophys. Res. Lett., 35, L13810, https://doi.org/10.1029/2008GL033968, 2008.

Massoli, P., Onasch, T.B., Cappa, C.D., Nuamaan, I., Hakala, J., Hayden, K., Li, S.M., Sueper, D.T., Bates, T.S., Quinn, P.K., Jayne, J.T., Worsnop, D.R.: Characterization of black carbon-containing particles from soot particle aerosol mass spectrometer measurements on the R/V Atlantis during CalNex 2010, J. Geophys. Res.- Atmos., 120, 2575-2593, https://doi.org/10.1002/2014JD022834, 2015.

Rose, D., Gunthe, S. S., Mikhailov, E., Frank, G. P., Dusek, U., Andreae, M. O., and Pöschl, U.: Calibration and measurement uncertainties of a continuous-flow cloud condensation nuclei counter (DMT-CCNC): CCN activation of ammonium sulfate and sodium chloride aerosol particles in theory and experiment, Atmos. Chem. Phys., 8, 1153–1179, https://doi.org/10.5194/acp8-1153-2008, 2008.